Scavenger Receptor Cysteine-Rich domains of Lysyl Oxidase-Like2 regulate endothelial ECM and angiogenesis through non-catalytic scaffolding mechanisms

Claudia Umana-Diaz, Cathy Pichol-Thievend, Marion F Marchand, Yoann Atlas, Romain Salza, Marilyne Malbouyres, Alain Barret, Jérémie Teillon, Corinne Ardidie-Robouant, Florence Ruggiero, et al.

Scavenger Receptor Cysteine-Rich domains of Lysyl Oxidase-Like2 regulate endothelial ECM and angiogenesis through non-catalytic scaffolding mechanisms

Claudia Umana-Diaz[a,b,3], Cathy Pichol-Thievend[a,b,1,4], Marion F. Marchand[a,b,1], Yoann Atlas[a,b], Romain Salza[c], Marilyne Malbouyres[d], Alain Barret[a], Jérémie Teillon[a,5], Corinne Ardidie-Robouant[a], Florence Ruggiero[d], Catherine Monnot[a], Philippe Girard[e,f], Christophe Guilluy[g], Sylvie Ricard-Blum[c], Stéphane Germain[a,2] and Laurent Muller[a,2]

a - Center for Interdisciplinary Research in Biology (CIRB), *Collège de France, CNRS, INSERM, PSL Research University, Paris, France*
b - Sorbonne Université, *Collège Doctoral, Paris, France*
c - University Claude Bernard Lyon 1, *CNRS, INSA Lyon, CPE, Institute of Molecular and Supramolecular Chemistry and Biochemistry, UMR, 5246, Villeurbanne, France*
d - Institut de Génomique Fonctionnelle (IGFL), *ENS-Lyon, UMR CNRS, 5242, Université de Lyon, Lyon, France*
e - Institut Jacques Monod, *UMR7592 CNRS, Université Paris Diderot, Sorbonne Paris Cité, Paris, France*
f - Biomedical and Fundamental Science Faculty, *Université Paris Descartes, Sorbonne Paris Cité, Paris, France*
g - Institute for Advanced Biosciences, *INSERM U1209, CNRS UMR 5309, Université Grenoble Alpes, La Tronche, France*

Correspondence to Laurent Muller: *Center for Interdisciplinary Research in Biology, Collège de France, Paris, 11 Place Marcelin Berthelot, F-75005, France.* *laurent.muller@college-de-france.fr*
https://doi.org/10.1016/j.matbio.2019.11.003

Abstract

Lysyl oxidases are major actors of microenvironment and extracellular matrix (ECM) remodeling. These cross-linking enzymes are thus involved in many aspects of physiopathology, including tumor progression, fibrosis and cardiovascular diseases. We have already shown that Lysyl Oxidase-Like 2 (LOXL2) regulates collagen IV deposition by endothelial cells and angiogenesis. We here provide evidence that LOXL2 also affects deposition of other ECM components, including fibronectin, thus altering structural and mechanical properties of the matrix generated by endothelial cells. LOXL2 interacts intracellularly and directly with collagen IV and fibronectin before incorporation into ECM fibrillar structures upon exocytosis, as demonstrated by TIRF time-lapse microscopy. Furthermore, surface plasmon resonance experiments using recombinant scavenger receptor cysteine-rich (SRCR) domains truncated for the catalytic domain demonstrated their direct binding to collagen IV. We thus used directed mutagenesis to investigate the role of LOXL2 catalytic domain. Neither enzyme activity nor catalytic domain were necessary for collagen IV deposition and angiogenesis, whereas the SRCR domains were effective for these processes. Finally, surface coating with recombinant SRCR domains restored deposition of collagen IV by LOXL2-depleted cells. We thus propose that LOXL2 SRCR domains orchestrate scaffolding of the vascular basement membrane and angiogenesis through interactions with collagen IV and fibronectin, independently of the enzymatic cross-linking activity.

Introduction

Lysyl oxidases (LOX and LOX-Like 1 to 4) are responsible for the covalent cross-linking of ECM proteins and participate to the remodeling of the microenvironment associated with tissue development and pathologies including cardiovascular diseases, fibrosis and cancer [1,2]. These copper-dependent enzymes catalyze the deamination of hydroxylysines and lysines in collagens and elastin.

They all share the copper-binding residues and the catalytic tyrosine and lysine that form the lysyl tyrosylquinone cofactor (LTQ) (Fig. S4A). This family of enzymes is subdivided in two groups that differ in the degree of conservation of both the catalytic and the N-terminal domains [3]. LOX and LOXL1 share 88% similarity in the catalytic domain. They have unique N-terminal domains that act as propeptides whose cleavage is required for activation of the amine oxidase activity. Whereas the catalytic domains of LOXL2-4 also share 86−88% similarity, they only have 64−68% similarity with the catalytic domains of LOX and LOXL1. In addition, LOXL2-4 share a common specific structure of their N-terminus consisting in 4 repeats of scavenger receptor cysteine rich (SRCR) domains whose function remains quite elusive. SRCR domains are ancient and highly conserved domains of 100−115 residues characterized by 3 or 4 intradomain disulfide bonds that are present in secreted and cell surface proteins associated with pattern recognition of extracellular proteins [4]. LOXL2 has mainly been associated with pathological microenvironments in fibrosis and cancer because of its increased expression and of the impact of its inhibition on disease progression in animal models [5−7]. Whereas oxidation of collagen I and tropoelastin by LOXL2 had been described for long, it is only recently that their LOXL2-mediated cross-linking has been demonstrated [8,9]. Similarly, LOXL2-mediated cross-linking of collagen IV, which had already been proposed [10,11], was only recently demonstrated [12]. Interactions of LOXL2 that do not involve catalytic activity have also been recently identified, including with other ECM components like ADAMTS10 and ADAMTSL2, and fibulins [13,14], further suggesting that LOXL2 could be involved in elastogenesis [15]. In addition to ECM remodeling, a non-collagenous substrate of LOXL2 has been proposed to affect tumor progression through the regulation of the paracrine PDGF-AB signaling pathway [16]. Finally, intracellular functions of LOXL2 have also been proposed, mainly in the context of tumor progression and epithelial-mesenchymal transition through the regulation of Snail [17,18]. Even though LOXL2 was a promising therapeutic target in fibrosis and cancer, recent clinical trials using a LOXL2 specific antibody inhibiting enzyme activity did not prove up to the expectations [2,19,20].

LOXL2 was also described as a regulator of the cardiovascular system both during development and in extracellular matrix cardiovascular disease like aneurysm [21−23]. Gene deletion of *LOXL2* in mouse results either in defects in the development of the cardiovascular system associated to partial [24] or complete lethality [25], whereas aged heterozygous LOXL2$^{+/-}$ mice are protected from vascular stiffening [25]. LOXL2 was identified as one of the most up-regulated genes in endothelial tip cells during retina vascularization [26] and its expression follows growth of intersomitic vessels (ISV) during zebrafish embryo development [10]. The involvement of LOXL2 in the regulation of angiogenesis has been demonstrated in physiological [10] and pathological contexts [27−29]. Sprouting angiogenesis, the formation of new blood vessels budding from pre-existing ones, involves proliferation and migration of endothelial cells, as well as capillary morphogenesis [30]. These processes are associated with extensive remodeling of the microenvironment, including degradation of the pre-existing extracellular matrix (ECM) and *de novo* generation of the vascular basement membrane [31]. Basement membrane provides the only structural support to capillaries, as these vessels lack a smooth muscle wall, and participates to neovessel stabilization and pericyte recruitment. It thus regulates dynamic processes including cell adhesion, migration and survival, as well as signaling. We have reported that LOXL2 is co-localized with collagen IV in the basement membrane of newly formed capillaries in the retina of newborn rat [10], and LOXL2 is indeed considered as part of the machinery involved in formation of the collagen IV core of the basement membrane [32]. The involvement of collagen IV in the regulation of sprouting angiogenesis was demonstrated by defects in brain microvasculature detected in collagen IV-deficient mouse embryos, even though deposition of other basement membrane components and formation of large vessels were not affected [33].

Basement membrane is a complex network of entangled self-assembled macromolecular complexes that require organization into supra-structures for achieving its multifunctional biologic roles [34,35]. Interaction of ECM-associated proteins with the core of basement membrane remains poorly understood, even though their role is essential for capillary formation, as demonstrated for fibronectin [36,37]. We have previously shown that LOXL2 depletion in endothelial cells resulted in defects in collagen IV deposition *in vitro* that were correlated with inhibition of capillary formation in 3D angiogenesis models and during zebrafish embryo development. The effect of LOXL2 depletion was however not mimicked by inhibition of lysyl oxidase enzyme activity, neither *in vitro* nor in zebrafish embryos [10], suggesting that non-catalytic activity of LOXL2 was involved in ECM organization and/or angiogenesis. In the present paper, we have thus investigated the role of LOXL2 domains in the organization of the vascular ECM and how they impact the formation of ISV during zebrafish development, and of capillaries *in vitro.* Altogether, our data demonstrated that the SRCR domains of LOXL2 alone are effective for both ECM scaffolding and 3D capillary morphogenesis, whereas its catalytic activity is not necessary for these processes.

Results

LOXL2 regulates deposition of ECM components through direct interactions

We have already shown that LOXL2 is co-localized with collagen IV and fibronectin in fibrillar structures of the ECM deposited *in vitro* by endothelial cells, but not with the matricellular protein Cyr61 [10]. Depleting LOXL2 in these cells resulted in defects in collagen IV deposition in the ECM without altering mRNA synthesis and secretion of the protein [10]. We here investigated the impact of LOXL2 depletion on deposition of other basement membrane components. Endothelial cells were seeded at confluency and maintained for 2 and 3 days prior to immunofluorescence or extraction of ECM proteins for immunoblotting, respectively (Fig. 1). Perlecan and fibronectin deposition was strongly affected, whereas laminin deposition was inhibited by only 25%, as assessed by western blotting. These

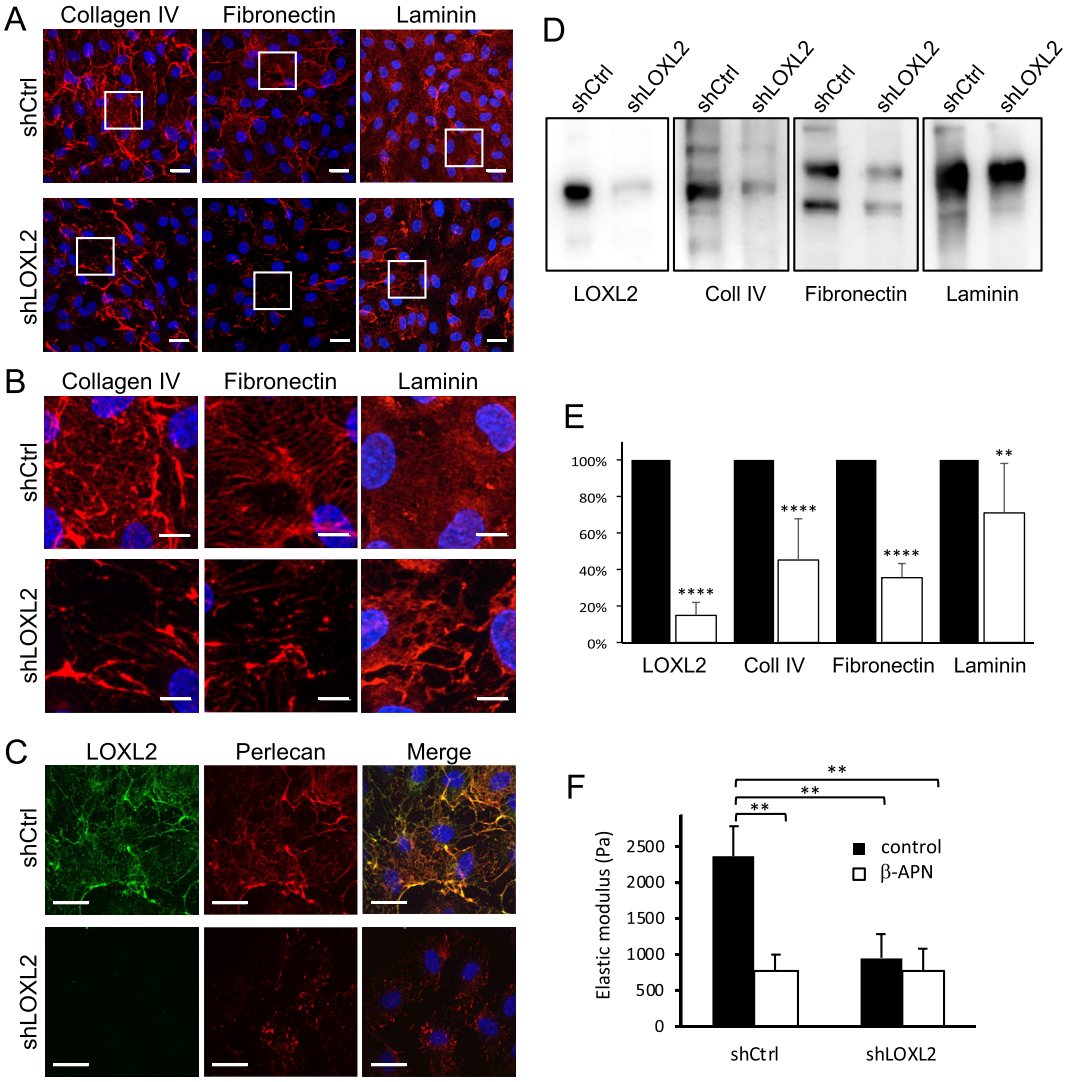

Fig. 1. LOXL2 regulates the deposition of ECM proteins. A–**C**: Control (shCtrl) and LOXL2-depleted (shLOXL2) endothelial cells were seeded on coverslips. Immunostaining of perlecan, collagen IV, fibronectin, and laminin was performed 48 h after seeding. Nuclei were stained with DAPI. Boxed areas are illustrated in **B**. Bars: 25 μm (**A** and **C**) and 10 μm (**B**). **D** and **E**: ECM proteins from endothelial cells cultured for 72 h were solubilized and separated by SDS-PAGE. LOXL2, collagen IV, fibronectin and laminin were immunodetected (**D**). Amounts of each protein in the ECM of control (black box) and LOXL2-depleted (white box) cells was normalized to the mean of controls (**E**). Graph presents the mean of 4 independent experiments. Values are presented ± SD. $^{**}P < 0.005$ and $^{****}P < 0.0001$. (**F**) The stiffness of cell-derived matrix was measured using atomic force microscopy. Graph presents the mean of 3 independent experiments. Values are presented ± SD. $^{**}P < 0.005$.

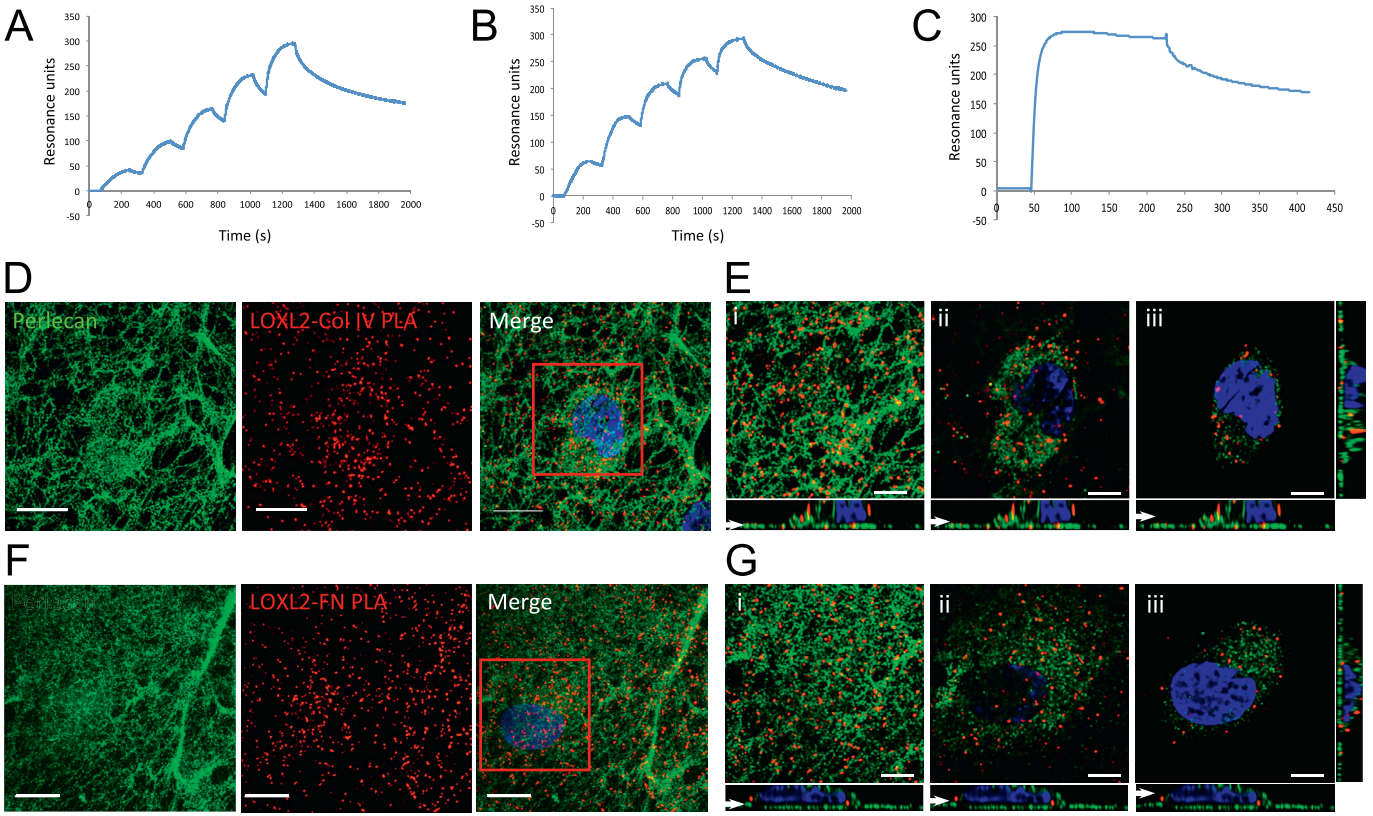

Fig. 2. LOXL2 directly interacts with collagen IV and fibronectin intracellularly prior to incorporation in the ECM upon exocytosis. A–**C**: LOXL2 directly binds to collagen IV and fibronectin. Several concentrations of full-length LOXL2 ((8, 16, 32, 64 and 128 nM - **A**) or SRCR12 (62.5, 125, 250, 500 nM and 1 μM - **B**) were injected at 30 μL/min for 180s over immobilized collagen IV. 500 nM LOXL2 was injected at 30 μL/min over immobilized fibronectin (**C**). **D-G**: Subcellular distribution of the interactions of LOXL2 with collagen IV and fibronectin. PLA was performed for analysis of the distribution of LOXL2 interactions with collagen IV (**D** and **E**) or fibronectin (**F** and **G**) on confluent endothelial cells that had deposited ECM. PLA signal (red) corresponding to LOXL2 interactions was analyzed by confocal microscopy. **D** and **F** display z projections of the whole stacks. Boxed areas are presented in **E** and **G**, which display 3 z-planes (**i-iii**) and the orthogonal views. White arrows indicate the z positions of the 3 single planes above. Perlecan immunostaining (green) was used to localize the ECM layer (**i**) and nuclei staining with DAPI to localize the intracellular layer (**iii**). Bar: 10 μm **(D** and **F**), and 5 μm **(E** and **G**). The 3D reconstructions are presented in the online movies 1 (for collagen IV) and 2 (for fibronectin). **H** and **I:** Incorporation of LOXL2-GFP in the ECM was followed by time-lapse TIRF microscopy. **H**: A mixed population of confluent endothelial cells expressing or not LOXL2-GFP was imaged 24 h after seeding. Two cells expressing LOXL2-GFP sequentially migrate in the field of view. Arrows indicate the edge of each cell (the first in green, and the second in red). Arrowheads indicate stable fibrillar structures that have incorporated LOXL2-GFP, with a similar color-code as for the cells. Time is indicated in minutes. Bar: 20 μm. See online movie 3. **(I)** An isolated migrating cell was imaged 24 h after seeding. GFP fluorescence is illustrated at the starting point (0' - green) and after 15 min (red). The merged image illustrates ECM remodeling associated to cell migration: LOXL2 is incorporated into nascent fibrillar structures at the migration front. White arrow indicates the direction of migration (top row). Bar: 10 μm. A zoomed area (white box) illustrates incorporation of LOXL2-GFP in nascent fibrillar structures (arrows; bottom row). Time is indicated in minutes. Bar: 5 μm. See online movie 4.

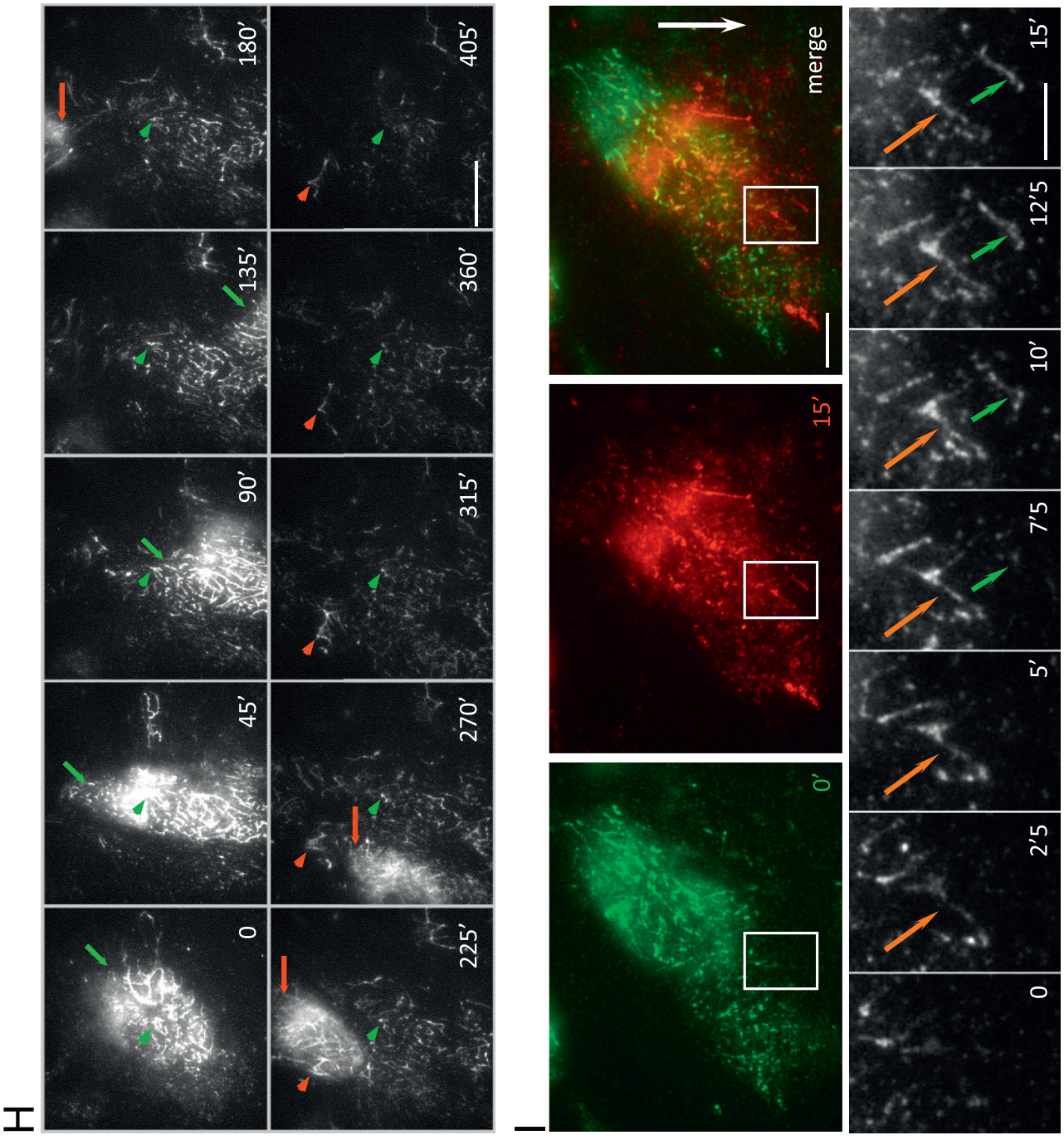

Fig. 2. (*continued*).

defaults of deposition of matrix proteins were not associated with down-regulation of their expression (Fig. S1). Furthermore, the fibronectin that was not deposited in the ECM was detected in the secretion medium as already described for collagen IV (Fig. S2) [10], suggesting that LOXL2-depletion affected their assembly in the ECM rather than their secretion. The stiffness of the ECM generated by endothelial cells was measured using atomic force microscopy. The defects in organization and composition of the ECM observed upon LOXL2 depletion were correlated with decreased stiffness to a comparable level as in the presence of β-APN, a pharmacological pan-inhibitor of lysyl oxidase activity (Fig. 1F).

Preliminary experiments analyzing the kinetics of co-localization of LOXL2 suggested that it was associated earlier and to a higher level with fibronectin than with collagen IV (Fig. S3). To gain insight into the mechanisms involved in the regulation of their deposition by LOXL2, we investigated direct interactions between these proteins using surface plasmon resonance (Fig. 2A–C). We characterized two binding sites of LOXL2 to collagen IV, including one of very high affinity, with equilibrium dissociation constants: $K_{D1} = 8.9 \pm 2.9$ nM and $K_{D2} = 0.016 \pm 0.009$ nM. The LOXL2-collagen IV interactions displayed the following association rates of 7.54E+05 Ms^{-1} and 4.93E+04 Ms^{-1}, and dissociation rates of 6.1E-03 s^{-1} and 7.47E-07 s^{-1}. We also investigated the interactions of a recombinant protein corresponding to the N-terminal SRCR domains 1 and 2 (SRCR12) (Fig. S4). We could detect direct binding of SRCR12 to collagen IV (Fig. 2B). SPR experiments also demonstrated the direct binding of LOXL2 to fibronectin (Fig. 2C). We could however not calculate kinetic parameters and affinity for these interactions since the signal decreased before the end of the association phase. We then investigated the subcellular distribution of the interactions of LOXL2 with these proteins using proximity ligation assay (PLA). The experimental conditions were first set up by quantifying PLA dots in isolated LOXL2-depleted endothelial cells for identification of specific interactions with collagen IV or fibronectin (Fig. S5). Using confocal microscopy, these interactions were then analyzed in confluent monolayers that had generated a polarized ECM. Most of the PLA signal was detected in the ECM focal planes, which were identified using perlecan as a marker. We also identified intracellular PLA dots corresponding to LOXL2-collagen IV and LOXL2-fibronectin interactions in the perinuclear region (Fig. 2D–G; movies 1 and 2).

Supplementary video related to this article can be found at https://doi.org/10.1016/j.matbio.2019.11.003.

The incorporation of LOXL2 in the ECM was further investigated by time-lapse TIRF microscopy. A mosaic population of cells expressing a LOXL2-GFP construct or not was cultured at confluency (Fig. 2H, Movie 3). LOXL2-GFP was directly incorporated in filamentous structures of the ECM underneath the endothelial cell expressing the chimera. Cells loaded the matrix locally as they migrated (Fig. 2H, arrows) without diffusion of LOXL2-GFP to the ECM located under the neighboring cells. After cells had passed through the field of view, an important pool of fluorescent LOXL2 was rapidly released from the matrix (within 10 min), whereas a smaller fraction of fluorescent LOXL2 remained bound to the ECM for several hours (Fig. 2H, arrowheads). These two pools of LOXL2-GFP could correspond to the two rates of dissociation of LOXL2 from collagen IV that were measured in SPR experiments. In order to investigate more precisely LOXL2 incorporation into the ECM, we acquired closer time-lapse images of migrating endothelial cells (Fig. 2I, Movie 4). LOXL2-GFP was deposited into nascent ECM fibrillar structures at the migration front. Incorporation in these fibrillar structures appeared as blinking spots of high intensity typical of exocytosis [38]. Altogether, these data suggest that LOXL2 has a scaffolding activity responsible for building up a network of macromolecules, including collagen IV and fibronectin, in the basement membrane.

Supplementary video related to this article can be found at https://doi.org/10.1016/j.matbio.2019.11.003.

LOXL2 catalytic activity is not required for collagen IV deposition and capillary formation

Considering the direct interaction of the SRCR domains with collagen IV, we then investigated whether LOXL2 function in ECM deposition requires its amine oxidase activity. We have already shown that pharmacological inhibition of lysyl oxidase activity by β-APN: i) does not affect collagen IV deposition in the ECM *in vitro*; -ii) only partially inhibits capillary formation in 3D assays; -iii) does not affect ISV formation in zebrafish embryo [10]. Considering the wide spectrum of inhibition of β-APN and the conflicting results concerning its efficacy in cell culture [3], we further investigated the involvement of LOXL2 catalytic activity using site directed mutagenesis. A point mutation of the tyrosine residue in the LTQ was generated (LOXL2-Y689A; Fig. S6) to inactivate the catalytic activity, as previously described for LOX [39]. The LOXL2-Y689A mutant was secreted by transfected CHO cells but inactive, as monitored by measuring the total ß-APN-sensitive lysyl oxidase activity in the secretion medium (Fig. 3A and B). We have already shown that transducing LOXL2-depleted cells with wild-type LOXL2 restored both ECM deposition and capillary formation [10]. We here performed similar

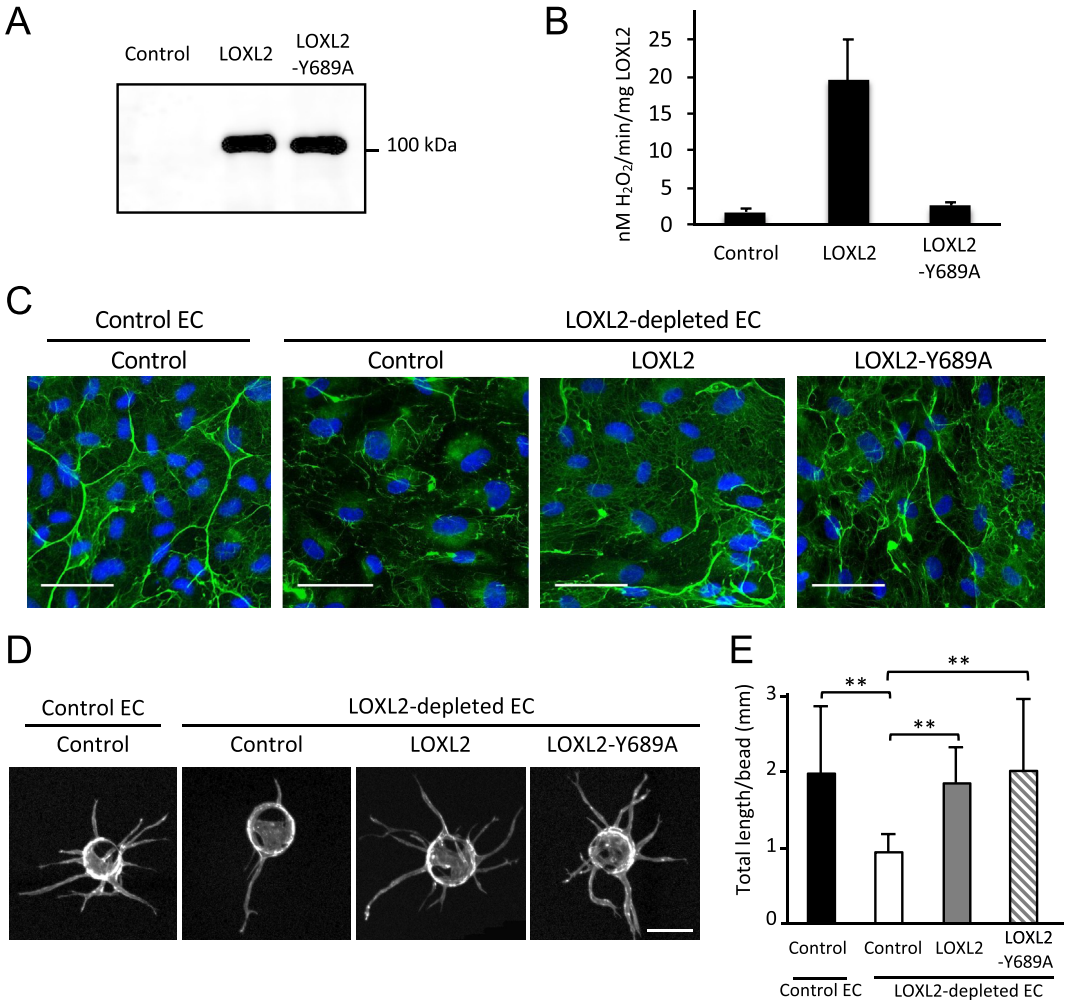

Fig. 3. LOXL2 catalytic activity is not necessary for collagen IV deposition and capillary formation. A and **B:** CHO cells were transfected with a control plasmid or with plasmids encoding either wild type LOXL2 or the Y698A mutant. Overnight secretion media were collected. Amounts of secreted LOXL2 were assessed by Western blot (**A**) and lysyl oxidase activity was measured (**B**). **C to E**: Control and LOXL2-depleted endothelial cells (EC) were transduced with lentivirus encoding either GFP (control) or LOXL2 or the LOXL2-Y689A mutant. **C**: Immunostaining of collagen IV was performed 5 days after seeding. Bar: 50 μm. **D** and **E**: Capillary formation was assessed after 6 days of culture using the cytodex bead assay. Bar: 200 μm. Capillary length was measured in 3 independent experiments of duplicate wells (**E**). Graph presents the mean value of total sprout length/bead ± SD. $^{**}P < 0.005$.

experiments using mutant LOXL2. The expression of wild type and mutant LOXL2 in endothelial cells was assessed by Western blot, using antibodies directed against either LOXL2 catalytic domain or the myc epitope tag in order to distinguish between endogenous and transduced LOXL2 (Fig. S6B). Similar levels of wild-type and Y689A mutant LOXL2 were detected. Cells expressing the different LOXL2 constructs were seeded at confluency in order to promote collagen IV deposition. Whereas deposition of collagen IV by LOXL2-depleted cells was inhibited, re-expressing LOXL2 reversed this effect (Fig. 3C). Collagen IV deposition by endothelial cells expressing the LOXL2-Y689A was also restored and displayed a similar distribution as when deposited by cells expressing wild-type LOXL2 (Fig. 3C). In vitro capillary formation in 3D fibrin hydrogels was also inhibited using LOXL2-depleted cells, and restored to control levels by wild type LOXL2 or LOXL2-Y689A (Fig. 3D and E).

A parallel approach based on re-expression of human LOXL2 was performed in LOXL2 knocked-down zebrafish embryos. ISV formation was altered upon LOXL2 depletion, resulting in misguiding of vessels and absence of dorsal longitudinal anastomotic vessel, as well as loss of connection with the aorta (Fig.4 Aii, and movie 5), and lack of perfusion of ISV (Fig. 4B). Co-injection of the mRNA encoding

wild-type human LOXL2 together with the translation morpholino that down-regulates endogenous LOXL2 rescued this phenotype, as previously described [10]. The involvement of LOXL2 catalytic activity in the regulation of angiogenesis was then investigated using an mRNA encoding the human LOXL2-Y689A mutant. ISV formation and perfusion were rescued to the same extent as with wild-type human mRNA (Fig. 4), suggesting that LOXL2 catalytic activity was not required.

Supplementary video related to this article can be found at https://doi.org/10.1016/j.matbio.2019.11.003.

The SRCR domains of LOXL2 are effective for collagen IV deposition and capillary formation

We then investigated the function of the different domains of LOXL2. In addition to the copper-binding site and LTQ, the catalytic domain contains a cytokine receptor-like domain (CRL) (Fig. S6A) whose function remains unknown. Moreover, processing of LOXL2 between SRCR domains 2 and 3 has been described [40,41], suggesting that these domains could be involved in different functions. We thus assessed the proteolytic processing of LOXL2 by endothelial cells using antibodies targeting the N- or C-terminus. These experiments revealed the presence of full length LOXL2 (105 kDa) together with processed forms not detected when cells were LOXL2-depleted (Fig. 5A): an N-terminal fragment of 37 kDa, and a complementary C-terminal fragment of 68 kDa. Both proteolytic fragments were detected in the ECM and the secretion medium, but absent from the cell extracts. Indeed, bands of smaller molecular weight were detected in cell lysates only with the C-terminal antibody, and those were not altered by shRNA targeting LOXL2. These data are consistent with the processing of LOXL2 by extracellular proprotein convertases releasing a molecular form consisting in SRCR domains 1 and 2 (SRCR12) [40,41]. The ratio of these proteolytic fragments to full length LOXL2 was higher in the ECM than in the secretion medium, but our experiments do not allow to distinguish between processing in the ECM or in the secretion medium.

LOXL2-depleted endothelial cells were transduced with lentiviruses encoding either wild type or SRCR12 or SRCR14 forms of LOXL2. Expressing any of these three forms restored collagen IV deposition in the ECM (Fig. 5B), even though SRCR12 and SRCR14 did not reach as high levels of expression as full length LOXL2 (Fig. S6). The three constructs also restored capillary formation to the same extent as control cells (Fig. 5C), demonstrating that the two N-terminal SRCR domains are sufficient for collagen IV deposition and capillary formation *in vitro*.

In order to perform a similar investigation in zebrafish embryos, two complementary approaches were used: i) injection of a splicing morpholino; and −ii) co-injection of a translation morpholino with an mRNA. A splicing morpholino targeting the sequence joining intron 8 and exon 9, thus splicing exon 9, was designed to result in the insertion of a stop codon in the open reading frame, and thus in translation of a protein truncated for the whole catalytic domain. Splicing of LOXL2 mRNA was confirmed by RT-PCR (Fig. 6A). The only antibody directed against LOXL2 that recognizes the zebrafish protein, in our hands, targets the catalytic domain. Investigating deletion of the catalytic domain by Western blot using this antibody resulted in loss of the band present in control embryos and absent in embryos injected with a translation morpholino (Fig. 6B). Vessel formation and perfusion were restored in 77.8% of zebrafish embryos expressing truncated LOXL2 (Fig. 6C and D). We also co-injected the translation morpholino with an mRNA encoding human LOXL2 deleted for its catalytic domain (SRCR14). Semi-quantitative RT-PCR revealed that similar amounts of the injected mRNA were still present at 10 and 22 h post-fertilization (hpf) (Fig. 6E), demonstrating the presence of Loxl2a mRNA at the developmental stage of ISV growth. We could however not detect the truncated human LOXL2 using an antibody directed against the myc epitope. Nevertheless, formation and perfusion were completely rescued in 63%, and partially rescued in 19% of LOXL2-SRCR14 injected embryos (Fig. 6F and G; movie 5). These data demonstrate that the catalytic domain is not required for deposition of collagen IV in the ECM and formation of capillaries.

LOXL2 regulates ECM deposition in a context-dependent manner

We further characterized the ECM scaffolding function of LOXL2 using recombinant full length and truncated forms of LOXL2 as surface coating. Secretion and proper glycosylation profile of the recombinant proteins were verified by SDS-PAGE, suggesting the correct folding of these proteins (Fig. S4). Control and LOXL2-depleted endothelial cells were seeded in tissue culture dishes coated or not with the recombinant proteins and collagen IV deposition was analyzed by immunofluorescence 3 days after seeding (Fig. 7A). All three forms of LOXL2 restored collagen IV deposition. The pattern of collagen IV was however lacking the thick filamentous material that was generated by endothelial cells in the absence of coating. These data showed that LOXL2 and its two N-terminal SRCR domains could provide binding sites for collagen IV, as suggested by the direct interaction between these

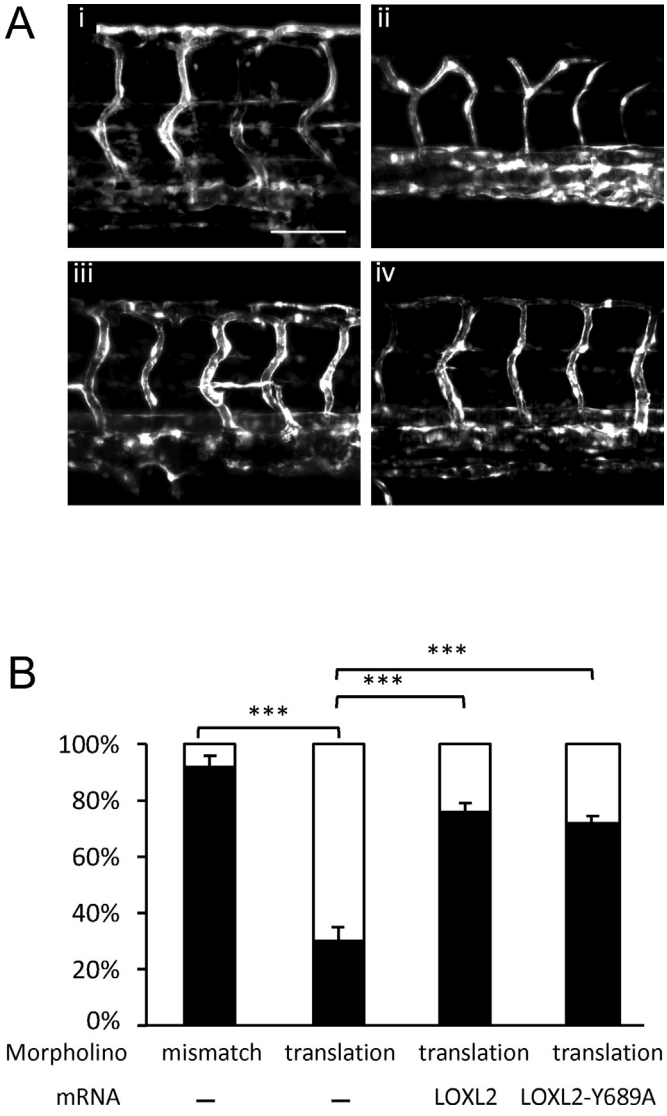

Fig. 4. LOXL2 catalytic activity is not necessary for ISV formation. A and **B**: Zebrafish embryos were co-injected with a mismatch morpholino (i) or a morpholino targeting LOXL2 translation (ii-iv), and co-injected with an mRNA encoding either human wild type LOXL2 (iii) or the Y689A catalytic site mutant of human LOXL2 (iv). **A**: Capillary formation was analyzed in tg(fli1:EGFP)y^{1} zebrafish embryos by lightsheet microscopy. Bar: 100 μm **B**: ISV displaying blood circulation were counted at 72 hpf. Graph presents the quantification of embryos displaying less (black box) and more (white box) than 5 non-circulating ISV of 5 independent experiments ± SD. ***$P < 0.0001$.

proteins. A similar pattern of collagen IV deposition lacking large fibrillar structures was also observed when endothelial cells were seeded on collagen I or fibronectin (Fig. 7B). Under such culture conditions, LOXL2 followed the same pattern of deposition as collagen IV: the large fibrillar structures detected when cells were seeded in the absence of coating were lost when cells were seeded on fibronectin or collagen I (Fig. 7B). Quite remarkably, LOXL2 depletion only altered collagen IV deposition in the absence of coating (Fig. 7C-left column) but did not affect the fine and homogenous distribution of collagen IV in the ECM when endothelial cells were seeded on collagen I or fibronectin (Fig. 7C- middle and right column). These data suggest that LOXL2 is part of large macromolecular complexes of ECM proteins whose deposition is mutually relying on the presence of one of the components in the ECM.

Discussion

Morphogenetic processes are tightly regulated by remodeling of the microenvironment, including

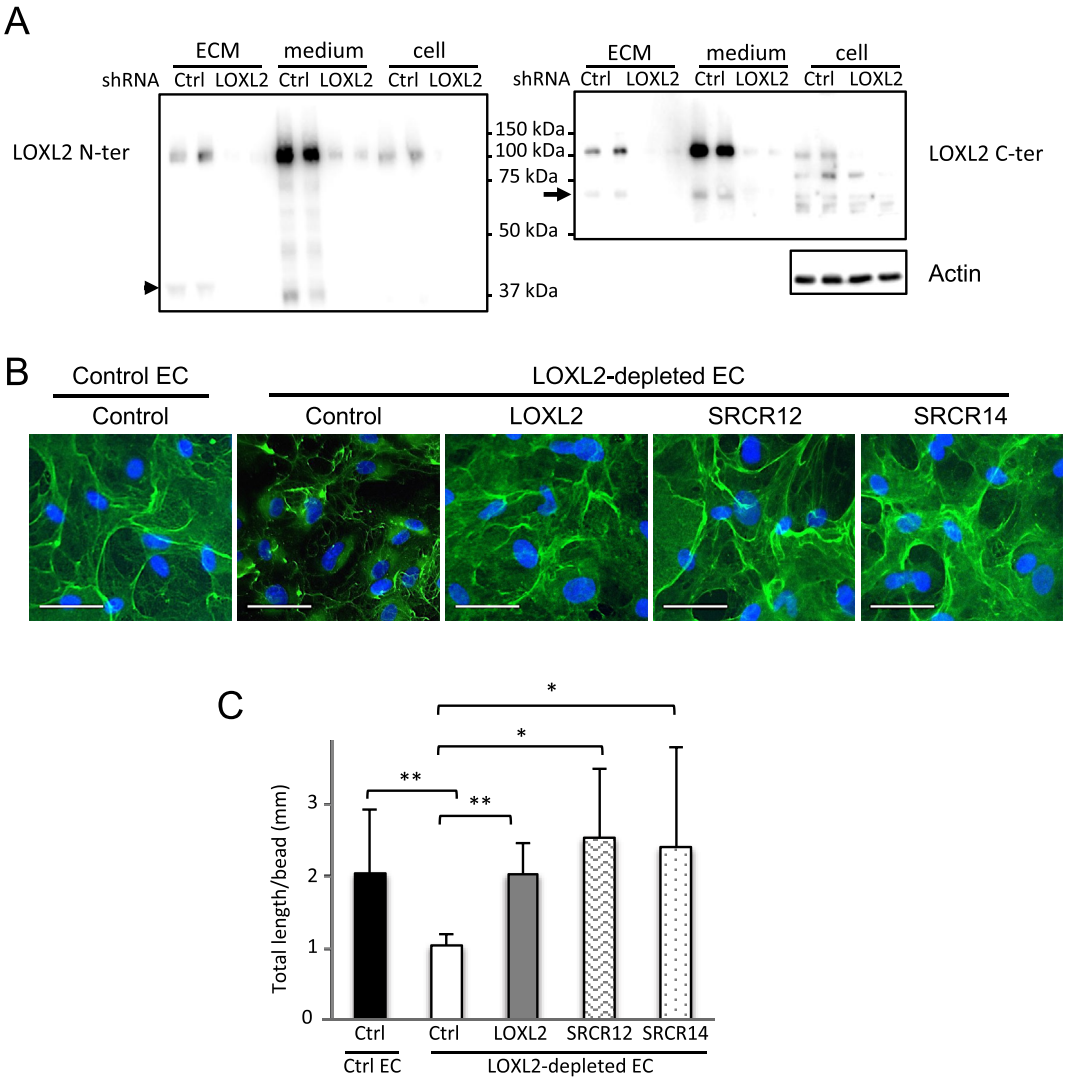

Fig. 5. LOXL2 SRCR domains are effective for collagen IV deposition and capillary formation. A: Overnight medium of control and LOXL2-depleted cells was collected, and cell and ECM lysates were prepared. Proteins from duplicate culture wells were separated by SDS-PAGE and LOXL2 was identified by Western blot using antibodies directed against either the N-terminus (left panel) or the C-terminal catalytic domain (top right panel). Arrowhead indicates the N-terminal 42 kDa fragment, and arrow indicates the 65 kDa C-terminal fragment. Similar amounts of proteins were loaded on both gels. Actin was detected in cell lysates as a loading control (bottom right panel). **B**: Control and LOXL2-depleted endothelial cells (EC) were transduced with lentivirus encoding either GFP (control) or LOXL2 or LOXL2 deleted for the catalytic domain and SRCR domains 3 and 4 (SRCR12) or for the catalytic domain only (SRCR14). Immunostaining of collagen IV was performed 5 days after seeding. Bar: 25 μm **C**: Capillary formation was assessed after 6 days of culture using the cytodex bead assay. Sprout length was measured in 3 independent experiments performed in duplicate wells. Graph presents the mean value of total sprout length/bead ± SD. *$P < 0.05$ and **$P < 0.005$.

composition and physical properties of basement membrane [35,42]. Sprouting angiogenesis indeed requires *de novo* building of the vascular basement membrane at the surface of growing capillaries, as demonstrated for several components, including collagen IV [33] and fibronectin [37]. We have previously demonstrated the impact of LOXL2 depletion on collagen IV deposition and angiogenesis [10]. We here describe impairment of the deposition of fibronectin and perlecan, suggesting that LOXL2 acts as a key regulator of the organization of the vascular basement membrane. Our data also demonstrate that the catalytic activity of LOXL2 is not involved in these processes. Using a structure-function approach, we actually found that LOXL2 SRCR domains alone play a central role in ECM generation and capillary formation. Our data thus suggest that LOXL2 could act as a scaffolding

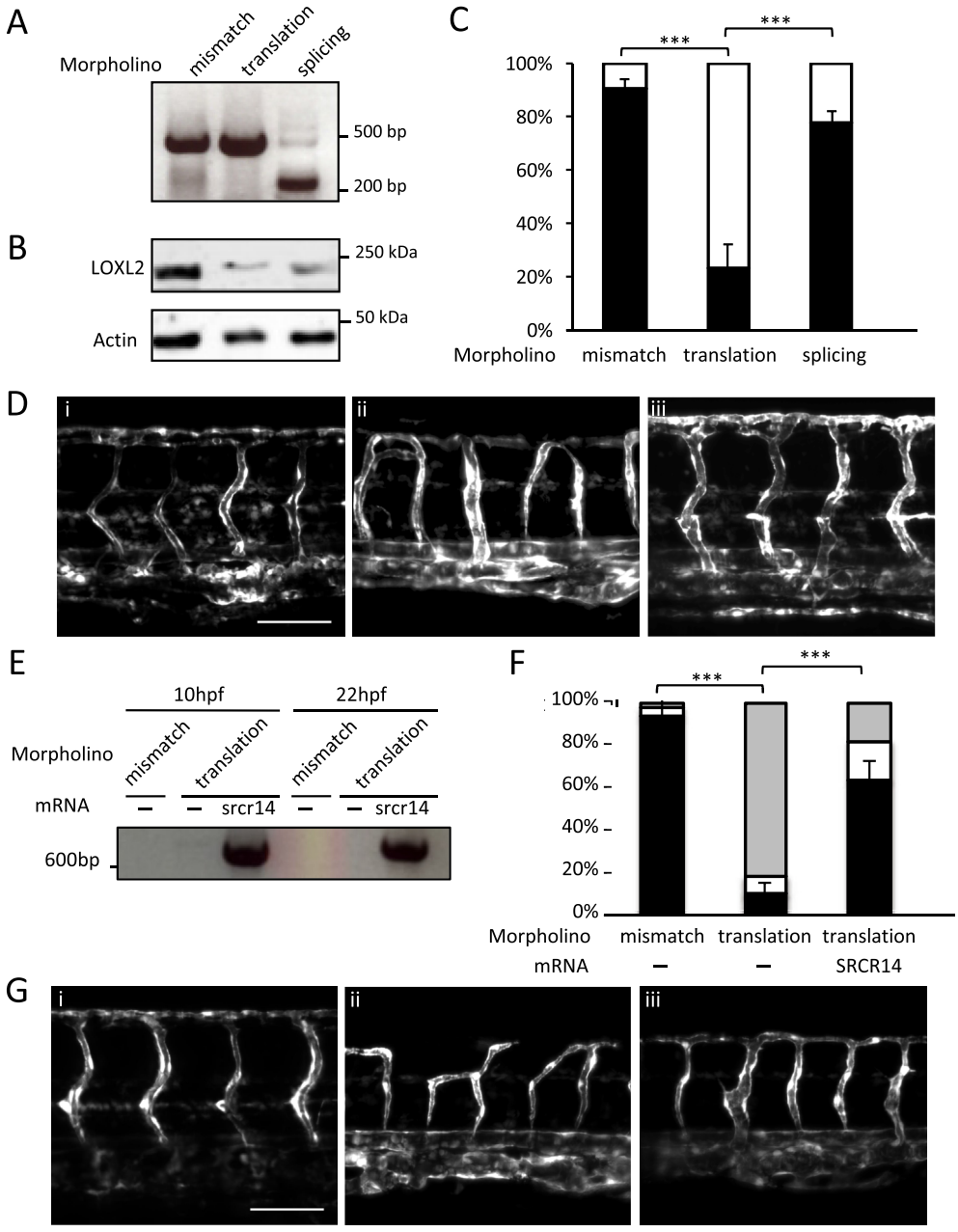

Fig. 6. LOXL2 SRCR domains regulate ISV formation in zebrafish embryo. A-D. Zebrafish embryos were injected with a mismatch (i) or a translation morpholino targeting LOXL2 (ii), or a splicing morpholino targeting exon 9 (iii). Splicing of loxl2 was verified by RT-PCR (**A**) and deletion of the catalytic domain was confirmed by Western blot using an antibody directed against the catalytic domain (**B**). ISV displaying blood circulation were counted at 72 hpf (**C**). Graph presents the quantification of embryos displaying less (black box) and more (white box) than 5 non-circulating ISV of 4 independent experiments ± SD. ***$P < 0.0001$. Capillary formation was investigated in tg(fli1:EGFP)y^1 zebrafish embryos by lightsheet microscopy. Bar: 100 μm (**D**). **E-G**. Zebrafish embryos were injected with mismatch (i) or translation morpholino targeting LOXL2 (ii), and co-injected with an mRNA encoding human LOXL2 deleted for the catalytic domain (SRCR14) (iii). Amount of human mRNA was assessed by RT-PCR (**E**). ISV displaying blood circulation were counted at 72 hpf (**F**). Embryos were distributed in three groups displaying less than 5 (black box), 5 to 10 (white bow) or more than 10 (grey box) non-circulating ISV. Graph presents the mean value of 5 independent experiments ± SD. ***$P < 0.0001$. **G**: Capillary formation was investigated in tg(fli1:EGFP)y^1 zebrafish embryos by lightsheet microscopy. Bar: 100 μm.

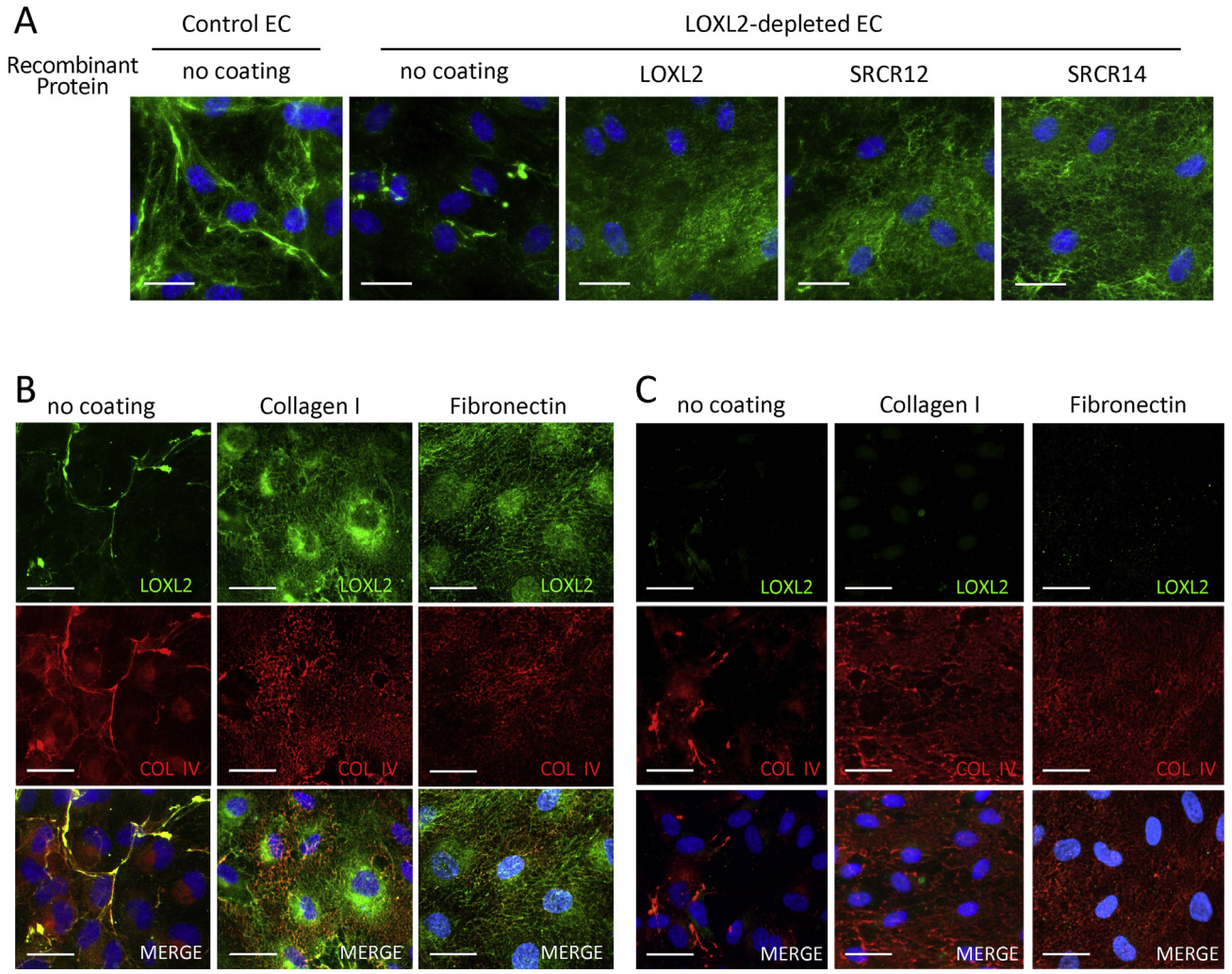

Fig. 7. Surface coating promotes Collagen IV deposition by LOXL2-depleted cells. A: Control and LOXL2-depleted endothelial cells (EC) were seeded either without coating or after coating of the culture dish with recombinant LOXL2, or SRCR12 or SRCR14 proteins. Immunostaining of collagen IV was performed 3 days after seeding. Nuclei were stained with DAPI. **B** and **C**: Control and LOXL2-depleted cells were seeded either without coating or after coating of the culture dish with either collagen I or fibronectin. Immunostaining of LOXL2 and collagen IV was performed 3 days after seeding. Nuclei were stained with DAPI. Bar: 25 μm.

protein participating to the macromolecular organization of the ECM, thus providing the appropriate microenvironment to blood vessels.

Organization of the vascular basement membrane is mediated by the autocrine deposition of ECM components by endothelial cells. Whereas some proteins like laminins and collagen IV undergo self-assembly, the key components and mechanisms that regulate the organization of these macromolecules into supra-structures remain largely unknown. LOXL2 could be a regulator of this process as its depletion alters deposition of several components and mechanical properties of the ECM generated by endothelial cells. Such scaffolding activity would then be completed by LOXL2-mediated crosslinking of collagen IV [32]. A similar function was described for LOX in elastogenesis, as it binds both fibulin-4 and tropoelastin, which is then a substrate for LOX [43]. We detected direct and intracellular interactions of LOXL2 with collagen IV and fibronectin. Progression of collagen IV from the endoplasmic reticulum to secretory vesicles requires post-translational modifications including hydroxylation of lysines and prolines [42], and is regulated by the intracellular specific chaperones HSP47 and Tango1 [44,45]. An appealing hypothesis would be that LOXL2 interacts with the trimeric protomer of collagen IV in the late secretory pathway, and acts as a specific chaperone prior to deposition in the ECM network. Since processing of the SRCR domains is required for cross-linking of collagen IV [40], the N-terminal SRCR domains 1 and 2 could protect collagen IV from premature cross-linking in the secretory pathway, thus promoting the correct formation of the 7S domain in the ECM. Such chaperone activity associated with post-Golgi intracellular trafficking and conserved through evolution has been proposed for other secreted enzymes and for SPARC interaction with collagen IV [46,47]. Antibodies specific for the NC1 and 7S domains of collagen a3a4a5 (IV) demonstrated the polarized deposition of collagen IV in the basement membrane, with the 7S pointing to the interstitial matrix [48]. Interaction of LOXL2 with the 7S domain [12] could thus participate to such molecular polarization in the basement membrane. We also detected intracellular and direct interactions of LOXL2 with fibronectin. Binding of fibronectin to LOX catalytic domain had already been described [49]. This interaction was critical for LOX activation even though fibronectin was not a substrate for LOX. Together with the early and high co-localization of LOXL2 and fibronectin in the ECM, these data suggest that a complex between these two proteins could participate in organization of the endothelial ECM.

Whereas the core machinery involved in the trafficking of basement membrane components starts to be established, the mechanisms involved in sorting and targeting these cargo proteins remain unknown [42]. TIRF microscopy demonstrated that LOXL2 was directly incorporated upon exocytosis into the basal ECM underneath the secreting cell, corresponding to the polarized deposition of ECM. Hot spots of exocytosis appeared to be distributed along filamentous structures, demonstrating intracellular targeting of LOXL2 to the sites of its deposition. Furthermore, LOXL2 was incorporated within the fibrillar structures of the ECM, rather than at their tip, suggesting that it added up proteins in these structures rather than participated to their elongation. In addition, persistence of part of the LOXL2-GFP signal in the ECM for hours after secretion could correspond to the cross-linking of this enzyme to collagen IV [40].

Knocking-down Loxl2a expression in zebrafish embryo altered ISV formation, whereas β-APN had no effect. β-APN also hardly inhibited *in vitro* capillary formation by HUVEC [10]. Mutation of the LTQ did not affect capillary formation *in vivo* and *in vitro* either. Similar mutations also had no effect on other LOXL2-mediated functions [11], including regulation of epithelial [50] or endothelial [29] to mesenchymal transition or expression of cell polarity factors [51] or keratinocyte differentiation [52]. In this latter study, an antibody targeting SRCR domain 4 however inhibited LOXL2 impact on differentiation, suggesting that protein interactions of the SRCR domains could be mediating LOXL2 effect. In our study, complete deletion of the catalytic domain further demonstrated the lack of involvement of the enzyme activity, and ruled out the possibility that LOXL2 acts through the CRL domain. Interestingly, intracellular activity of LOXL2 SRCR domains was also demonstrated through their interaction with GATA6 [53].

Propeptides of enzymes are known to regulate their catalytic activity, either by intramolecular promotion of the folding of the catalytic site and/or by inhibition of the enzyme activity [54,55]. Similar function holds true for LOX and LOXL1 propeptides [56,57], but not for LOXL2, as processing of its propeptide is not associated with activation of the amine oxidase activity [40,41]. Other roles have been proposed for processed propeptides of lysyl oxidases, and are still under investigation [43]. Unlike LOX and LOXL1, LOXL2 propeptide is actually not cleaved off from the catalytic domain, but processed in two halves, which releases only the 2 N-terminal SRCR domains (SRCR12). Our recent SAXS and electron microscopy analyses of LOXL2 structure revealed that only SRCR4 is interacting with the catalytic domain, and that the SRCR domains are organized in a string of pearl manner that supports processing and release of SRCR12 domains [9]. This fragment was not detected in endothelial cell lysates, but was naturally occurring after secretion, in agreement with its generation by extracellular serine proteases [40,41]. After

secretion SRCR12 was in both the medium and the ECM, where the ratio of SRCR12 to full length LOXL2 was the highest. We also demonstrated the direct interaction of SRCR12 with collagen IV using SPR. Whereas we did not succeed in expressing the two N-terminal SRCR domains alone in zebrafish embryo, using either splicing morpholino or injection of mRNA, SRCR12 was successfully expressed in endothelial cells and mimicked LOXL2 impact on matrix deposition and capillary formation. Finally, collagen IV deposition by LOXL2-depleted cells was restored when culture support was coated with SRCR12. A general feature of SRCR domains is binding to cell surface and ECM molecules through wide spectrum pattern recognition [3], and dimerization of class A SRCR domains is particularly adapted to recognition of large ligands [58], which corresponds to the proposed interaction between LOXL2 SRCR domains and the 7S domain of collagen IV. These data thus support a novel function for LOXL2 SRCR domains as scaffolding domains in the ECM.

Many mechanisms have been proposed explaining the impact of LOXL2 on cell behavior [3], including through expression of Snail [17,50] or activation of FAK/Src [29,59], both through catalytic or non−catalytic mechanisms. In endothelial cells, intracellular LOXL2 also regulates gene expression through direct interaction of intracellular LOXL2 with GATA6-AS [60]. These authors demonstrated that these effects are distinct from the regulation of angiogenesis, which only involves extracellular LOXL2. Another recent study proposes that LOXL2 and its enzyme-dead mutant regulate similarly the endothelial to mesenchymal transition [29]. The non-catalytic regulation of basement membrane deposition by LOXL2 that we describe fits quite well with these hypotheses. Scaffolding of collagen IV and fibronectin by the ECM-localized LOXL2 could thus play a major role in angiogenesis considering the importance of cell-mediated remodeling of the basement membrane for acquisition of function [42]. Inactivation of genes encoding collagen a1(IV) and collagen a2(IV) in mouse resulted in inhibition of sprouting angiogenesis in the developing brain [33]. Fibronectin is also required for angiogenesis, and more particularly cellular fibronectin released by endothelial cells in a polarized and autocrine manner [61,62]. In addition, direct interactions of fibronectin with collagen IV have been known for long and more recent studies have proposed that fibronectin fibrillogenesis is required for collagen IV deposition [63,64]. A complex involving collagen IV, fibronectin and LOXL2 at the interface between endothelial cells and interstitial ECM could thus be required for regulation of angiogenesis. Altogether, our data extend the catalytic function of LOXL2 in biosynthesis of the collagen IV core [32] to a wider role as a non-catalytic scaffolding organizer in the basement membrane at its interface with ECM.

The non-catalytic mechanisms that we identified could participate to the development of pathologies of the vascular basement membrane, including intracranial and retinal aneurysms [21−23]. Such mechanisms should therefore be considered in the context of inhibitor development, especially after failure of recent clinical trials targeting LOXL2 catalytic activity [2,19,20]. Indeed, collagen IV mutations impact the endothelium function in pathologies including small vessel diseases, which are associated with tortuous blood vessels, hemorrhages and aneurysms [65]. Even though collagen IV is present in the basement membrane in these pathologies, transmission electron microscopy reveals interruptions and dilations of the vascular basement membranes. Affecting LOXL2 function in the organization of the vascular basement membrane could thus have long-term effects on endothelial integrity and function.

Experimental procedures

Antibodies and reagents

LOXL2 antibodies were purchased from Cell Signaling Technology (rabbit mAb #69301) (Boston, MA, USA.) and Abnova (mouse mAb #H00004017-M01) (Heidelberg, Germany); type IV collagen antibodies from Novotec (rabbit polyclonal #20411) (Lyon, France); anti-myc clone 9E10 mouse mAb # 11-667-203-001), fluorescent secondary antibodies, DAPI, Amplex Red were purchased from Life Technologies (Carlsbad CA, USA); fibrinogen (#341578) and thrombin (#605190) from Calbiochem/merck (Darmstadt, Germany), VEGF (#293-VE-050) from R&D, horseradish peroxidase, 1,5-diaminopentane and β-APN from Sigma-Aldrich (Saint-Louis, MO, USA).

Cell culture

Human umbilical vein endothelial cells (HUVEC) were prepared and grown as previously described [66] in endothelial cell growth medium (ECGM2). Experiments were performed using HUVEC between passages 2 and 5. Normal human dermal fibroblasts were purchased from Promocell (Heidelberg, Germany) and grown in Fibroblast Growth Medium 2 (Promocell).

Immunofluorescence

Confluent (40,000 cells/cm^2) cells were seeded on glass coverslips or in 6 channels ibiTreat microslides ibidi® (Martinsried, Germany) and cultured for 2−5 days before fixation with 4% paraformaldehyde and permeabilization with Triton-X-100 (0.5%). In some experiments, coverslips were coated with 230 μM of recombinant protein (full length LOXL2-myc-His, LOXL2-SRCR14-myc-His, LOXL2-SRCR12-myc-His) for 1 h at 37 °C. Primary and secondary antibodies were incubated in the presence of 1% normal goat serum. Coverslips were mounted in

Mowiol and for 6 channels ibidi micro-slides, liquid mounting medium was added into each channel. Images were acquired with a spinning disk confocal microscope equipped with an HQ2 coolsnap camera using a 63× objective (Nikon-Roper).

Protein extraction and immunoblotting

For cell lysate, confluent HUVECs were directly extracted with Laemmli buffer containing DTT (50 mM) before separation by SDS-PAGE. For HUVEC ECM proteins, cells were detached on ice with 0.5% DOC, washed with PBS prior to similar protein extraction. For secreted protein, overnight serum-free ECGM2 was collected and centrifuged. Proteins were precipitated with 1% TCA followed with acetone and ether washes, before treatment with Laemmli buffer.

For zebrafish analysis, 10 dechorionated embryos were lysed in 25 mM Tris pH 7.5, 100 mM NaCl, 5 mM EDTA, 0,5% DOC, 0,5% NP40® containing protease inhibitor cocktail (Sigma-Aldrich). Lysates were centrifuged 15 min at 15000 rpm and pellets were solubilized in Laemmli buffer containing DTT.

Proteins were then separated by SDS-PAGE and transferred to PVDF membranes before incubation with the appropriate antibodies in 25 mM Tris-HCl, pH 7.4, 0.1% Tween 20, and 5% milk. Immunological detection was performed with streptavidin-horseradish peroxidase (HRP) conjugated secondary antibodies, using ECL (Life-Technologies) as a substrate.

Atomic force microscopy

Matrix stiffness was determined by probe force spectroscopy using an atomic force microscope (NanoWizard 3, JPK Instruments, Berlin, Germany) placed on a vibration isolation table. A silicon nitride cantilever with conical tip (0.06 N/m) was used. Exact spring constant was determined upon calibration in PBS by the thermal noise method prior to each experiment. We used the Young's modulus of the endothelial ECM as a measurement of matrix elasticity. AFM force-distance curves were transformed to force-indentation curves and fitted using the JPK data processing software. Automated curve fitting was applied using the first 500 nm of indentation as a fitting range, and using the contact-point independent linear Hertz-Sneddon model modified for a cone [67].

SPR binding assays

SPR binding assays were carried out in a Biacore T100 system (GE Healthcare, Protein Science Facility, UMS 3444, Lyon, France) using human placenta collagen IV and human plasma fibronectin (C7521 and F2006, Sigma). They were covalently immobilized on a dextran-covered CM5 sensor chip using the amine coupling kit (GE Healthcare) according to the manufacturer's instructions at a flow rate of 5 μL/min with 10 mM Hepes, 150 mM NaCl, P20 0.05% pH 7.4 as runining buffer. The carboxyl groups of CM5 sensor chips were activated by injecting N-hydroxysuccinimide/1-ethyl-3-(3-dimethylaminopropyl) carbodiimide for 420 s. Ligands were injected for 420 s at 100 μg/mL over the activated sensor chip. The residual activated groups were blocked by injecting 1 M ethanolamine pH 8.5 for 420 s. Two injections of running buffer of 60 s each were then performed. The immobilization levels were 4039 RUs for collagen IV and 3000 RUs for fibronectin.

Several concentrations of full-length LOXL2 (8, 16, 32, 64 and 128 nM) and SRCR12 domains (62.5, 125, 250, 500 nM and 1 μM) were injected at 30 μl/min for 180s over immobilized ligands and over a control flow cell submitted to the coupling steps without ligand to evaluate non specific binding, which was subtracted from raw data. The association (ka) and dissociation rate (kd) constants and the equilibrium dissociation constant (KD) were calculated using the Biaevaluation software (version 2.0.3).

Proximity ligation assay (PLA)

Proximity ligation assay was performed using the Duolink® In Situ Red Starter Kit mouse/rabbit (Sima-Aldrich) following the manufacturer's instructions. Briefly, HUVEC were grown on 6-channel micro-slides (Ibidi, Martinsried, Germany). Cells were washed once with PBS, fixed with 4% paraformaldehyde in PBS and permeabilized with TritonX-100 (0.5%). LOXL2 was detected with a primary rabbit anti−human antibody (Cell signaling technologies), while collagen IV and fibronectin were detected using mouse anti−human antibodies (Millipore). The kit provided the corresponding probes of anti-rabbit PLUS and anti-mouse MINUS. Nuclei were then stained with DAPI containing mounting medium. Stacks of 26−30 images with a 300 nm step were acquired with a Nikon Ti-Roper iLas confocal spinning disk microscope, equipped with an HQ2 cool snap camera with a 100× objective.

TIRF microscopy

LOXL2-GFP cells were seeded in a glass bottom micro-dish (Ibidi, Martinsried, Germany) in ECGM2. Cells were maintained in an environmental control system at 37 °C, 5% CO_2 (Life Imaging System, Basel, Switzerland) and imaged after 24 or 48 h. One solid-state laser line (488 nm) was coupled to a TIRF condenser and time-lapse images were collected with a Nikon Ti-Roper iLas TIRF microscope, equipped with an Evolve EMCCD camera (Roper Scientific, Evry, France).

Expression vector, lentivirus, and shRNA tools

cDNA encoding human wild-type and mutant LOXL2 constructs were cloned in pLenti6/V5-DEST using the Gateway LR clonaseTM II (Life Technologies, Grand Island, NY, USA).

HUVEC from each umbilical cord were infected with non-targeting (control) or LOXL2 shRNA. Plasmids encoding shRNA were purchased from Sigma-Aldrich. Lentiviral production was performed using Mission lentiviral packaging mix (Sigma-Aldrich) according to the manufacturer's instructions. For rescue experiments, these cells were super-transduced with virus encoding Green Fluorescent Protein (GFP), LOXL2-GFP, wild-type LOXL2, catalytic

site mutant LOXL2-Y689A, LOXL2-SRCR14 (without catalytic domain) and LOXL2-SRCR12 (without catalytic domain and SRCR 3 and 4). These constructs were silently mutated at the shRNA recognition site. Transductions were repeated using HUVEC from different umbilical cords. Transduced cells were selected for 7 days with puromycin (2 μg/mL) for shRNA-mediated down-regulation and with blasticidin (2 μg/mL) for re-expression.

Lysyl oxidase activity assay

Lysyl oxidase activity was determined using cadaverine as a substrate in a fluorescent assay based on oxidation of Amplex Red to resorufin [68]. Overnight secretion medium from cells expressing wild-type LOXL2 or the catalytic mutant LOXL2-Y689A were incubated in 1.2 M urea, 0.05 M sodium borate, pH 8.2, 1 unit/mL horseradish peroxidase, 10 mM Amplex red, 10 mM of cadaverin at 37 °C for 1 h. Lysyl oxidase activity was calculated as the difference between total amine oxidase and the activity measured in the presence of 500 μM β-APN.

3D capillary formation assay

Three-dimensional fibrin gel assays were carried out as previously described [69]. Briefly, HUVEC were seeded on cytodex beads (GE Healthcare) 24 h before embedding in a 2.5 mg/mL fibrin gel. In some experiments, 230 μM recombinant LOXL2 proteins (LOXL2, LOXL2-SRCR14, LOXL2-SRCR12) were added to the hydrogels. Normal human dermal fibroblasts were plated on top of the gel. Capillaries were allowed to grow for 5–6 days in the presence of complete medium containing 10 ng/mL VEGF. Hydrogels were then fixed with 4% paraformaldehyde, stained with phalloidin-Alexa Fluor 488 and imaged with a Nikon Ti-Roper iLas confocal spinning disk microscope equipped with an HQ2 cool snap camera using a 10× objective (Nikon-Roper). Total tube length per bead was measured using ImageJ.

Downregulation of Loxl2a and ISV analysis in zebrafish embryo

Wild-type, Tg(fli1:EGFP)y[1] and Tg(kdrl:EGFP) zebrafish embryos were maintained according to common practices at 28 °C in embryo medium. Four ng of the translation morpholino targeting *loxl2a* or a control morpholino or a splicing morpholino targeting exons 5 and 6 of *loxl2a*, were microinjected into one-to two-cell stage embryos as previously described. Morpholinos were purchased from Gene Tools, LLC (Philomath, OR, USA). The following primers were used to detect splicing: forward 5′-AGCTGTAGACTAGGCAAAGCT-3’; reverse: 5′-CCATTTGAAGGACGTGTGGAA -3’.

For mRNA injection, 100 ng of each mRNA coding for LOXL2, LOXL2-Y689A or SRCR14-LOXL2, were co-microinjected into one-to two-cell stage embryos with 4 ng of the translation morpholino. The following primers were used to detect *srcr14-loxl2* mRNA: forward 5′-GACCGTCTGCGACGACAAG-3’; reverse 5′-GGTGATGATGACCGGTATGC-3’. Morphology of capillaries was investigated at 72 hpf using a home-built digital scanned laser light sheet microscope (DSLM) based on Keller and collaborators report [70] using a single illumination. Embryos were mounted in 1% low-melting agarose in a glass capillary (2 mm diameter) and extruded in an immersion chamber with a transferpettor piston (Brand, Wertheim, Germany). Samples were excited at 488 nm (Coherent, USA) with a 10×/0.3 objective lens (Leica, Germany). The focal plane of a 20×/0.5 U–V–I water-immersion objective lens (Leica, Germany) was imaged onto an sCMOS Orca Flash4 2.0 camera (Hamamatsu, Japan) through emission filter (Semrock, Rochester, NY, USA). Sample was moved using three motorized linear stage (M-111.1DG) and one rotative stage (M-660.55) (Physik Instrumente, Karlsruhe, Germany) controlled with custom-made software written in Labview (National Instruments, Austin, TX, USA). Stacks of 200-300 slices were processed with Fiji and orientated using the Interactive Stack Rotation plugin [71]. Images are presented as the maximum intensity projection of one half of the embryo.

Recombinant protein purification

The cDNA encoding either full length human LOXL2 or forms consisting of the four or two N-terminal SRCR domains were inserted in pcDNA3.1-myc-His at HindIII and XbaI restriction sites. PCR fragments were generated using the following primers: 5′-AAGCTTATGGAGAGGCCTCTG-3′ and 5′-TCTAGACTGCGGGGACAGCTG-3′ for LOXL2, 5′-TCTAGAGGTTTCTGAGCAGGC-3′ for SRCR14 and 5′-TCTAGAGAATCTTGAGGGTCC-3′ for SRCR12. Co-expression in dihydrofolate reductase-deficient CHO cells with the *dhfr* gene was performed using lipofectamine 2000 according to the manufacturer recommendations (Thermo Fischer Scientific, Waltham, MA). High expression clones were generated by serial subcloning in the presence of increasing concentrations of methotrexate (Sigma-Aldrich, St Louis,MO). Production and purification of recombinant proteins was performed on HisTrap columns (GE Healthcare, Pittsburgh, PA) as previously described [9].

Statistics

Statistical analysis of data was performed with Student t-test, unless otherwise stated and considered significant when P value < 0.05 (GraphPad Prism 4, GraphPad Software). Error bars represent the standard deviation.

Acknowledgements

We thank Yves Dupraz for fabrication of parts of the lightsheet microscope, Matthieu Boukaissi and Christine Rampon from the zebrafish facility, and Carole Gauron for help with zebrafish injections, and Sabrina Martin for RT-qPCR experiments.

Appendix A. Supplementary data

Supplementary data to this article can be found online at https://doi.org/10.1016/j.matbio.2019.11.003.

Funding

Building the lightsheet microscope was supported by grants from Fondation pour la Recherche Médicale (DBS20131128438) and ANR PulpCell to LM. AFM was acquired through an ERPT grant from Fondation Leducq to SG.

SPR assays were supported by grants from Fondation pour la Recherche Médicale (DBI20141231336 to SRB).

CUD was supported by Ministère de l'enseignement et de la Recherche. CPT was supported by Association pour la Recherche sur le Cancer (ARC); MFM by Fondation pour la Recherche Médicale (FRM); YA by la Ligue Nationale contre le Cancer.

Author contributions

Conceptualization: CUD, CPT, LM - Investigation: CUD, CPT, MFM, YA, RS, MM, AB, CAR - Methodology: YA, JT, PG, MFM - Visualization: CUD, YA, MFM, SRB - Funding acquisition: SG, LM - Writing: Original draft: LM - Review and editing: SRB, PG, MFM, CM, SG.

Competing financial interests

Authors declare no competing financial interests.

Received 8 August 2019;
Received in revised form 8 November 2019;
Accepted 12 November 2019
Available online 20 November 2019

Keywords:
Lysyl oxidase;
Angiogenesis;
ECM organization;
Vascular basement membrane;
Microenvironment remodeling

[1] Contributed equally as second author to this work.
[2] Contributed equally as last author to this work.
[3] CUD is now at INSERM U944, CNRS UMR7212, Institut Universitaire d'Hématologie, Sorbonne Paris Cité, Université Paris Diderot, Hôpital St. Louis, Paris, France.
[4] CPT is now at Institut Curie, PSL Research University, INSERM U1021, CNRS UMR3347, Orsay, France.
[5] JT is now at Bordeaux Imaging Center, Photonic Unit, Bordeaux, France, France.

References

[1] J.M. Mäki, Lysyl oxidases in mammalian development and certain pathological conditions, Histol. Histopathol. 24 (2009) 651–660.
[2] P.C. Trackman, Lysyl oxidase isoforms and potential therapeutic opportunities for fibrosis and cancer, Expert Opin. Ther. Targets 20 (2016) 935–945.
[3] H.J. Moon, J. Finney, T. Ronnebaum, M. Mure, Human lysyl oxidase-like 2, Bioorg. Chem. 57 (2014) 231–241.
[4] V.G. Martínez, S.K. Moestrup, U. Holmskov, J. Mollenhauer, F. Lozano, The conserved scavenger receptor cysteine-rich superfamily in therapy and diagnosis, Pharmacol. Rev. 63 (2011) 967–1000.
[5] V. Barry-Hamilton, R. Spangler, D. Marshall, S. McCauley, H.M. Rodriguez, M. Oyasu, A. Mikels, M. Vaysberg, H. Ghermazien, C. Wai, C.A. Garcia, A.C. Velayo, B. Jorgensen, D. Biermann, D. Tsai, J. Green, S. Zaffryar-Eilot, A. Holzer, S. Ogg, D. Thai, G. Neufeld, P. Van Vlasselaer, V. Smith, Allosteric inhibition of lysyl oxidase-like-2 impedes the development of a pathologic microenvironment, Nat. Med. 16 (2010) 1009–1017.
[6] J. Yang, K. Savvatis, J.S. Kang, P. Fan, H. Zhong, K. Schwartz, V. Barry, A. Mikels-Vigdal, S. Karpinski, D. Kornyeyev, J. Adamkewicz, X. Feng, Q. Zhou, C. Shang, P. Kumar, D. Phan, M. Kasner, B. López, J. Diez, K.C. Wright, R.L. Kovacs, P.S. Chen, T. Quertermous, V. Smith, L. Yao, C. Tschöpe, C.P. Chang, Targeting LOXL2 for cardiac interstitial fibrosis and heart failure treatment, Nat. Commun. 7 (2016) 13710.
[7] Y. Wei, T.J. Kim, D.H. Peng, D. Duan, D.L. Gibbons, M. Yamauchi, J.R. Jackson, C.J. Le Saux, C. Calhoun, J. Peters, R. Derynck, B.J. Backes, H.A. Chapman, Fibroblast-specific inhibition of TGF-β1 signaling attenuates lung and tumor fibrosis, J. Clin. Investig. 127 (2017) 3675–3688.
[8] H. Schilter, A.D. Findlay, L. Perryman, T.T. Yow, J. Moses, A. Zahoor, C.I. Turner, M. Deodhar, J.S. Foot, W. Zhou, A. Greco, A. Joshi, B. Rayner, S. Townsend, A. Buson, W. Jarolimek, The lysyl oxidase like 2/3 enzymatic inhibitor, PXS-5153A, reduces crosslinks and ameliorates fibrosis, J. Cell Mol. Med. 23 (2019) 1759–1770.
[9] C.E.H. Schmelzer, A. Heinz, H. Troilo, M.P. Lockhart-Cairns, T.A. Jowitt, M.F. Marchand, L. Bidault, M. Bignon, T. Hedtke, A. Barret, J.C. McConnell, M.J. Sherratt, S. Germain, D.J.S. Hulmes, C. Baldock, L. Muller, Lysyl oxidase-like 2 (LOXL2)-mediated cross-linking of tropoelastin, FASEB J. 33 (2019) 5468–5481.
[10] M. Bignon, C. Pichol-Thievend, J. Hardouin, M. Malbouyres, N. Bréchot, L. Nasciutti, A. Barret, J. Teillon, E. Guillon, E. Etienne, M. Caron, R. Joubert-Caron, C. Monnot, F. Ruggiero, L. Muller, S. Germain, Lysyl oxidase-like protein-2 regulates sprouting angiogenesis and type IV collagen assembly in the endothelial basement membrane, Blood 118 (2011) 3979–3989.

[11] P.C. Trackman, Enzymatic and non-enzymatic functions of the lysyl oxidase family in bone, Matrix Biol. 52–54 (2016) 7–18.
[12] C. Añazco, A.J. López-Jiménez, M. Rafi, L. Vega-Montoto, M.Z. Zhang, B.G. Hudson, R.M. Vanacore, Lysyl oxidase-like-2 cross-links collagen IV of glomerular basement membrane, J. Biol. Chem. 291 (2016) 25999–26012.
[13] R. Aviram, S. Zaffryar-Eilot, D. Hubmacher, H. Grunwald, J.M. Mäki, J. Myllyharju, S.S. Apte, P. Hasson, Interactions between lysyl oxidases and ADAMTS proteins suggest a novel crosstalk between two extracellular matrix families, Matrix Biol. 75–76 (2019) 114–125.
[14] T. Sasaki, F.G. Hanisch, R. Deutzmann, L.Y. Sakai, T. Sakuma, T. Miyamoto, T. Yamamoto, E. Hannappel, M.L. Chu, H. Lanig, K. von der Mark, Functional consequence of fibulin-4 missense mutations associated with vascular and skeletal abnormalities and cutis laxa, Matrix Biol. 56 (2016) 132–149.
[15] A.R.F. Godwin, M. Singh, M.P. Lockhart-Cairns, Y.F. Alanazi, S.A. Cain, C. Baldock, The role of fibrillin and microfibril binding proteins in elastin and elastic fibre assembly, Matrix Biol. (2019). [Epub ahead of print].
[16] F. Mahjour, V. Dambal, N. Shrestha, V. Singh, V. Noonan, A. Kantarci, P.C. Trackman, Mechanism for oral tumor cell lysyl oxidase like-2 in cancer development: synergy with PDGF-AB, Oncogenesis 8 (2019) 34.
[17] H. Peinado, M. Del Carmen Iglesias-de la Cruz, D. Olmeda, K. Csiszar, K.S. Fong, S. Vega, M.A. Nieto, A. Cano, F. Portillo, A molecular role for lysyl oxidase-like 2 enzyme in snail regulation and tumor progression, EMBO J. 24 (2005) 3446–3458.
[18] A. Millanes-Romero, N. Herranz, V. Perrera, A. Iturbide, J. Loubat-Casanovas, J. Gil, T. Jenuwein, A. García de Herreros, S. Peiró, Regulation of heterochromatin transcription by Snail1/LOXL2 during epithelial-to-mesenchymal transition, Mol. Cell 52 (2013) 746–757.
[19] D. Schuppan, M. Ashfaq-Khan, A.T. Yang, Y.O. Kim, Liver fibrosis: direct antifibrotic agents and targeted therapies, Matrix Biol. 68–69 (2018) 435–451.
[20] A.J. Muir, C. Levy, H.L.A. Janssen, A.J. Montano-Loza, M.L. Shiffman, S. Caldwell, V. Luketic, D. Ding, C. Jia, B.J. McColgan, J.G. McHutchison, G. Mani Subramanian, R.P. Myers, M. Manns, R. Chapman, N.H. Afdhal, Z. Goodman, B. Eksteen, C.L. Bowlus, GS-US-321-0102 investigators, simtuzumab for primary sclerosing cholangitis: phase 2 study results with insights on the natural history of the disease, Hepatology 69 (2019) 684–698.
[21] H. Akagawa, A. Narita, H. Yamada, A. Tajima, B. Krischek, H. Kasuya, T. Hori, M. Kubota, N. Saeki, A. Hata, T. Mizutani, I. Inoue, Systematic screening of lysyl oxidase-like (LOXL) family genes demonstrates that LOXL2 is a susceptibility gene to intracranial aneurysms, Hum. Genet. 121 (2007) 377–387.
[22] M. López-Luppo, V. Nacher, D. Ramos, J. Catita, M. Navarro, A. Carretero, A. Rodriguez-Baeza, L. Mendes-Jorge, J. Ruberte, Blood vessel basement membrane alterations in human retinal microaneurysms during aging, Investig. Ophthalmol. Vis. Sci. 58 (2017) 1116–1131.
[23] Y. Wu, Z. Li, Y. Shi, L. Chen, H. Tan, Z. Wang, C. Yin, L. Liu, J. Hu, Exome sequencing identifies LOXL2 mutation as a cause of familial intracranial aneurysm, World Neurosurg 109 (2018) e812–e818.
[24] A. Martin, F. Salvador, G. Moreno-Bueno, A. Floristán, C. Ruiz-Herguido, E.P. Cuevas, S. Morales, V. Santos, K. Csiszar, P. Dubus, J.J. Haigh, A. Bigas, F. Portillo, A. Cano, Lysyl oxidase-like 2 represses Notch1 expression in the skin to promote squamous cell carcinoma progression, EMBO J. 34 (2015) 1090–1109.
[25] J. Steppan, H. Wang, Y. Bergman, M.J. Rauer, S. Tan, S. Jandu, K. Nandakumar, S. Barreto-Ortiz, R.N. Cole, T.N. Boronina, W. Zhu, M.K. Halushka, S.S. An, D.E. Berkowitz, L. Santhanam, Lysyl oxidase-like 2 depletion is protective in age-associated vascular stiffening, Am. J. Physiol. Heart Circ. Physiol. 317 (2019) H49–H59.
[26] R. del Toro, C. Prahst, T. Mathivet, G. Siegfried, J.S. Kaminker, B. Larrivee, C. Breant, A. Duarte, N. Takakura, A. Fukamizu, J. Penninger, A. Eichmann, Identification and functional analysis of endothelial tip cell-enriched genes, Blood 116 (2010) 4025–4033.
[27] T. Van Bergen, R. Spangler, D. Marshall, K. Hollanders, S. Van de Veire, E. Vandewalle, L. Moons, J. Herman, V. Smith, I. Stalmans, The role of LOX and LOXL2 in the pathogenesis of an experimental model of choroidal neovascularization, Investig. Ophthalmol. Vis. Sci. 56 (2015) 5280–5289.
[28] S. Zaffryar-Eilot, D. Marshall, T. Voloshin, A. Bar-Zion, R. Spangler, O. Kessler, H. Ghermazien, V. Brekhman, E. Suss-Toby, D. Adam, Y. Shaked, V. Smith, G. Neufeld, Lysyl oxidase-like-2 promotes tumour angiogenesis and is a potential therapeutic target in angiogenic tumours, Carcinogenesis 34 (2013) 2370–2379.
[29] O.G. de Jong, L.M. van der Waals, F.R.W. Kools, M.C. Verhaar, B.W.M. van Balkom, Lysyl oxidase-like 2 is a regulator of angiogenesis through modulation of endothelial-to-mesenchymal transition, J. Cell. Physiol. 234 (2019) 10260–10269.
[30] M. Potente, H. Gerhardt, P. Carmeliet, Basic and therapeutic aspects of angiogenesis, Cell 146 (2011) 873–887.
[31] M. Marchand, C. Monnot, L. Muller, S. Germain, Extracellular matrix scaffolding in angiogenesis and capillary homeostasis, Semin. Cell Dev. Biol. 89 (2019) 147–156.
[32] K.L. Brown, C.F. Cummings, R.M. Vanacore, B.G. Hudson, Building collagen IV smart scaffolds on the outside of cells, Protein Sci. 26 (2017) 2151–2161.
[33] E. Pöschl, U. Schlötzer-Schrehardt, B. Brachvogel, K. Saito, Y. Ninomiya, U. Mayer, Collagen IV is essential for basement membrane stability but dispensable for initiation of its assembly during early development, Development 131 (2004) 1619–1628.
[34] W. Halfter, P. Oertle, C.A. Monnier, L. Camenzind, M. Reyes-Lua, H. Hu, J. Candiello, A. Labilloy, M. Balasubramani, P.B. Henrich, M. Plodinec, New concepts in basement membrane biology, FEBS J. 282 (2015) 4466–4479.
[35] A. Pozzi, P.D. Yurchenco, R.V. Iozzo, The nature and biology of basement membranes, Matrix Biol. 57–58 (2017) 1–11.
[36] E.L. George, E.N. Georges-Labouesse, R.S. Patel-King, H. Rayburn, R.O. Hynes, Defects in mesoderm, neural tube and vascular development in mouse embryos lacking fibronectin, Development 119 (1993) 1079–1091.
[37] X. Zhou, R.G. Rowe, N. Hiraoka, J.P. George, D. Wirtz, D.F. Mosher, I. Virtanen, M.A. Chernousov, S.J. Weiss, Fibronectin fibrillogenesis regulates three-dimensional neovessel formation, Genes Dev. 22 (2008) 1231–1243.
[38] D. Toomre, J.A. Steyer, P. Keller, W. Almers, K. Simons, Fusion of constitutive membrane traffic with the cell surface observed by evanescent wave microscopy, J. Cell Biol. 149 (2000) 33–40.

[39] S.X. Wang, M. Mure, K.F. Medzihradszky, A.L. Burlingame, D.E. Brown, D.M. Dooley, A.J. Smith, H.M. Kagan, J.P. Klinman, A crosslinked cofactor in lysyl oxidase: redox function for amino acid side chains, Science 273 (1996) 1078–1084.
[40] A.J. Lopez-Jimenez, T. Basak, R.M. Vanacore, Proteolytic processing of lysyl oxidase like-2 in the extracellular matrix is required for crosslinking of basement membrane collagen IV, J. Biol. Chem. 292 (2017) 16970–16982.
[41] K. Okada, H.J. Moon, J. Finney, A. Meier, M. Mure, Extracellular processing of lysyl oxidase-like 2 and its effect on amine oxidase activity, Biochemistry 57 (2018) 6973–6983.
[42] A.J. Isabella, S. Horne-Badovinac, Building from the ground up: basement membranes in Drosophila development, Curr. Top. Membr. 76 (2015) 305–336.
[43] P.C. Trackman, Functional importance of lysyl oxidase family propeptide regions, J Cell Commun Signal 12 (2018) 45–53.
[44] T. Marutani, A. Yamamoto, N. Nagai, H. Kubota, K. Nagata, Accumulation of type IV collagen in dilated ER leads to apoptosis in Hsp47-knockout mouse embryos via induction of CHOP, J. Cell Sci. 117 (2004) 5913–5922.
[45] D.G. Wilson, K. Phamluong, L. Li, M. Sun, T.C. Cao, P.S. Liu, Z. Modrusan, W.N. Sandoval, L. Rangell, R.A. Carano, A.S. Peterson, M.J. Solloway, Global defects in collagen secretion in a Mia3/TANGO1 knockout mouse, J. Cell Biol. 193 (2011) 935–951.
[46] I. Lindberg, B. Tu, L. Muller, I.M. Dickerson, Cloning and functional analysis of C. elegans 7B2, DNA Cell Biol. 17 (1998) 727–734.
[47] A. Chioran, S. Duncan, A. Catalano, T.J. Brown, M.J. Ringuette, Collagen IV trafficking: the inside-out and beyond story, Dev. Biol. 431 (2017) 124–133.
[48] W. Halfter, C. Monnier, D. Müller, P. Oertle, G. Uechi, M. Balasubramani, F. Safi, R. Lim, M. Loparic, P.B. Henrich, The bi-functional organization of human basement membranes, PLoS One 8 (2013), e67660.
[49] B. Fogelgren, N. Polgár, K.M. Szauter, Z. Ujfaludi, R. Laczkó, K.S. Fong, K. Csiszar, Cellular fibronectin binds to lysyl oxidase with high affinity and is critical for its proteolytic activation, J. Biol. Chem. 280 (2005) 24690–24697.
[50] E.P. Cuevas, G. Moreno-Bueno, G. Canesin, V. Santos, F. Portillo, A. Cano, LOXL2 catalytically inactive mutants mediate epithelial-to-mesenchymal transition, Biol. Open. 3 (2014) 129–137.
[51] G. Moreno-Bueno, F. Salvador, A. Martín, A. Floristán, E.P. Cuevas, V. Santos, A. Montes, S. Morales, M.A. Castilla, A. Rojo-Sebastián, A. Martínez, D. Hardisson, K. Csiszar, F. Portillo, H. Peinado, J. Palacios, A. Cano, Lysyl oxidase-like 2 (LOXL2), a new regulator of cell polarity required for metastatic dissemination of basal-like breast carcinomas, EMBO Mol. Med. 3 (2011) 528–544.
[52] J. Lugassy, S. Zaffryar-Eilot, S. Soueid, A. Mordoviz, V. Smith, O. Kessler, G. Neufeld, The enzymatic activity of lysyl oxidas-like-2 (LOXL2) is not required for LOXL2-induced inhibition of keratinocyte differentiation, J. Biol. Chem. 287 (2012) 3541–3549.
[53] T. Peng, X. Deng, F. Tian, Z. Li, P. Jiang, X. Zhao, G. Chen, Y. Chen, P. Zheng, D. Li, S. Wang, The interaction of LOXL2 with GATA6 induces VEGFA expression and angiogenesis in cholangiocarcinoma, Int. J. Oncol. 55 (2019) 657–670.
[54] R. Rozenfeld, L. Muller, S. El Messari, C. Llorens-Cortes, The C-terminal domain of aminopeptidase A is an intramolecular chaperone required for the correct folding, cell surface expression, and activity of this monozinc aminopeptidase, J. Biol. Chem. 279 (2004) 43285–43295.
[55] L. Muller, A. Cameron, Y. Fortenberry, E.V. Apletalina, I. Lindberg, Processing and sorting of the prohormone convertase 2 propeptide, J. Biol. Chem. 275 (2000) 39213–39222.
[56] M.V. Panchenko, W.G. Stetler-Stevenson, O.V. Trubetskoy, S.N. Gacheru, H.M. Kagan, Metalloproteinase activity secreted by fibrogenic cells in the processing of prolysyl oxidase. Potential role of procollagen C-proteinase, J. Biol. Chem. 271 (1996) 7113–7119.
[57] A. Borel, D. Eichenberger, J. Farjanel, E. Kessler, C. Gleyzal, D.J. Hulmes, P. Sommer, B. Font, Lysyl oxidase-like protein from bovine aorta. Isolation and maturation to an active form by bone morphogenetic protein-1, J. Biol. Chem. 276 (2001) 48944–48949.
[58] J.R. Ojala, T. Pikkarainen, A. Tuuttila, T. Sandalova, K. Tryggvason, Crystal structure of the cysteine-rich domain of scavenger receptor MARCO reveals the presence of a basic and an acidic cluster that both contribute to ligand recognition, J. Biol. Chem. 282 (2007) 16654–16666.
[59] H.E. Barker, D. Bird, G. Lang, J.T. Erler, Tumor-secreted LOXL2 activates fibroblasts through FAK signaling, Mol. Cancer Res. 11 (2013) 1425–1436.
[60] P. Neumann, N. Jaé, A. Knau, S.F. Glaser, Y. Fouani, O. Rossbach, M. Krüger, D. John, A. Bindereif, P. Grote, R.A. Boon, S. Dimmeler, The lncRNA GATA6-AS epigenetically regulates endothelial gene expression via interaction with LOXL2, Nat. Commun. 9 (2018) 237.
[61] B. Cseh, S. Fernandez-Sauze, D. Grall, S. Schaub, E. Doma, E. Van Obberghen-Schilling, Autocrine fibronectin directs matrix assembly and crosstalk between cell-matrix and cell-cell adhesion in vascular endothelial cells, J. Cell Sci. 123 (2010) 3989–3999.
[62] G. Mana, F. Clapero, E. Panieri, V. Panero, R.T. Böttcher, H.Y. Tseng, F. Saltarin, E. Astanina, K.I. Wolanska, M.R. Morgan, M.J. Humphries, M.M. Santoro, G. Serini, D. Valdembri, PPFIA1 drives active α5β1 integrin recycling and controls fibronectin fibrillogenesis and vascular morphogenesis, Nat. Commun. 7 (2016) 13546.
[63] C.G. Miller, A. Pozzi, R. Zent, J.E. Schwarzbauer, Effects of high glucose on integrin activity and fibronectin matrix assembly by mesangial cells, Mol. Biol. Cell 25 (2014) 2342–2350.
[64] M.S. Filla, K.D. Dimeo, T. Tong, D.M. Peters, Disruption of fibronectin matrix affects type IV collagen, fibrillin and laminin deposition into extracellular matrix of human trabecular meshwork (HTM) cells, Exp. Eye Res. 165 (2017) 7–19.
[65] M. Jeanne, D.B. Gould, Genotype-phenotype correlations in pathology caused by collagen type IV alpha 1 and 2 mutations, Matrix Biol. 57–58 (2017) 29–44.
[66] A. Cazes, A. Galaup, C. Chomel, M. Bignon, N. Bréchot, S. Le Jan, H. Weber, P. Corvol, L. Muller, S. Germain, C. Monnot, Extracellular matrix-bound angiopoietin-like 4 inhibits endothelial cell adhesion, migration, and sprouting and alters actin cytoskeleton, Circ. Res. 99 (2006) 1207–1215.
[67] P. Carl, H. Schillers, Elasticity measurement of living cells with an atomic force microscope: data acquisition and processing, Pflüg. Arch. 457 (2008) 551–559.

[68] A.H. Palamakumbura, P.C. Trackman, A fluorometric assay for detection of lysyl oxidase enzyme activity in biological samples, Anal. Biochem. 300 (2002) 245–251.
[69] N. Beckouche, M. Bignon, V. Lelarge, T. Mathivet, C. Pichol-Thievend, S. Berndt, J. Hardouin, M. Garand, C. Ardidie-Robouant, A. Barret, G. Melino, H. Lortat-Jacob, L. Muller, C. Monnot, S. Germain, The interaction of heparan sulfate proteoglycans with endothelial transglutaminase-2 limits VEGF165-induced angiogenesis, Sci. Signal. 8 (2015) ra70.
[70] P.J. Keller, A.D. Schmidt, J. Wittbrodt, E.H. Stelzer, Reconstruction of zebrafish early embryonic development by scanned light sheet microscopy, Science 322 (2008) 1065–1069.
[71] J. Schindelin, I. Arganda-Carreras, E. Frise, V. Kaynig, M. Longair, T. Pietzsch, S. Preibisch, C. Rueden, S. Saalfeld, B. Schmid, J.Y. Tinevez, D.J. White, V. Hartenstein, K. Eliceiri, P. Tomancak, A. Cardona, Fiji: an open-source platform for biological-image analysis, Nat. Methods 9 (2012) 676–682.